LIQUID CRYSTALS, 2016
VOL. 43, NOS. 13–15, 2051–2061
http://dx.doi.org/10.1080/02678292.2016.1191685

INVITED ARTICLE

Beam shaping via photopatterned liquid crystals

Peng Chen, Yan-Qing Lu and Wei Hu

National Laboratory of Solid State Microstructures, College of Engineering and Applied Sciences, and Collaborative Innovation Center of Advanced Microstructures, Nanjing University, Nanjing, China

ABSTRACT

Due to the fantastic properties and diverse applications of specific beams, optical beam shaping has attracted intensive attentions recently. Generally, these beams can be converted from Gaussian beams via particular spatial amplitude or phase control. In this work, we present a liquid crystal photopatterning technique based on dynamic microlithography with a polarisation-sensitive photoalignment agent. This technique enables the accurate, arbitrary and reconfigurable azimuthal angle control of liquid crystals, thus providing a powerful approach for the manipulation of light. By this means, the tailoring of arbitrary fine microstructures with binary or continuously space-variant liquid crystal azimuthal orientations are demonstrated. We briefly review our recent work on some specially designed patterns and corresponding specific optical fields. High-quality vortex beams, vector beams and Airy beams are generated with unprecedented flexibility in the design and control of light wavefront. Besides high efficiency, good electrical switchability and broad wavelength tolerance, the proposed devices also exhibit merits of compact size, low cost, dynamic mode conversion and polarisation controllable energy distribution, and are available for short pulse and intense light modulation. This work may pave a bright way towards beam shaping and bring new possibilities for the design of novel advanced liquid crystal photonic devices.

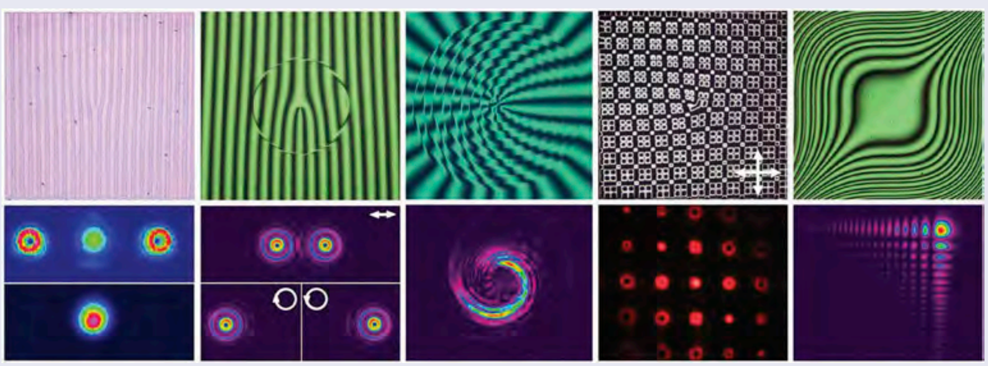

ARTICLE HISTORY
Received 20 April 2016

KEYWORDS
Liquid crystal; photopatterning; optical vortex; vector beam; Airy beam

1. Introduction

Optical beam shaping is a key requirement for optics and photonics. Recently, specific beams including vortex beams,[1,2] vector beams [3] and Airy beams [4] have been studied intensively due to their fantastic properties and diverse applications in optical trapping, laser processing, high-resolution imaging, etc. Generally, these beams can be generated by manipulation of multiple degrees of freedom of light such as particular spatial amplitude or phase control. Such manipulations could be accomplished via lens [5,6] or plates [7,8] of specific curvature radius, delicately structured photoresist masks [9–11] or metasurfaces.[12–14] Whereas, their optical characteristics are static, once the respective device is fabricated with a given set of dimensions. It severely restricts corresponding applications.

Owing to the excellent anisotropy and reconfigurability, liquid crystals (LCs) become the first choice for making these devices dynamic. The dominate liquid crystal displays (LCDs) can be considered as an example for intensity modulation in the visible range.[15,16] After introducing specially designed microstructures, LCs can manipulate both the polarisation and the spatial degrees of freedom of light. This brings LCs new possibilities beyond displays. Typically, polymer-dispersed LCs [17]

CONTACT Wei Hu huwei@nju.edu.cn National Laboratory of Solid State Microstructures, College of Engineering and Applied Sciences, and Collaborative Innovation Center of Advanced Microstructures, Nanjing University, Nanjing 210093, China

and patterned electrodes [18–20] have been adopted to locally and poloidally guide the LC directors to form binary phase patterns. Nevertheless, the manufacturing is complicated and the devices suffer from the problem of fixed structures. The microstructures could also be output by a spatial light modulator (SLM),[21] most of which consists of numerous discrete micro-size LC pixels driven separately. However, the complex electrode matrix makes the SLM costly and optically inefficient, and limits the quality of output beams. All above methods are based on the polar angle control of LCs, actually, the azimuthal angle could be employed as well. Micro-rubbing [22–24] and patterned rubbing [25,26] are adopted to carry out the patterned alignment. Compared to these mechanical methods, photoalignment is much more suitable for implementing accurate and high-resolution multi-domain LC alignments.[27,28] In the initial research, multi-step photolithography [28,29] and holography [30–33] are commonly utilised. More recently, several techniques exhibiting superior image-output flexibility are developed,[34–36] facilitating the realisations of complex LC orientations and subsequent optical characteristics. These techniques fully unlock a new degree of freedom to manipulate the directors of LCs. It might inspire emerging breakthroughs and next-generation innovations both in LCDs and non-display applications.

The past few years have witnessed the enormous progress in beam shaping based on LC photopatterning. In this article, we will review our recent works on this subject. We introduce the concepts of Pancharatnam–Berry phase and Dammann grating to design specific LC microstructures. With our previously developed dynamic photo patterning technique, corresponding fine microstructures with binary or space-variant LC azimuthal orientations are accomplished. Subsequently, novel optical fields such as optical vortices carrying arbitrary azimuthal/radial indices, equal-energy optical vortex arrays, complex vector beams and polarisation controllable Airy beams are accomplished and characterised. These systematic researches drastically extend the capability of optical field manipulation and may supply a promising approach for tailoring the wavefront.

2. Photoalignment technology and photopatterning system

Here, a polarisation-sensitive and photo-rewritable sulphonic azo-dye SD1 [37] is utilised as the photoalignment agent. Under linearly polarised UV exposure, the SD1 molecules tend to reorient their absorption oscillators perpendicular to the incident polarisation due to the isomerisation of azo groups and dichroic absorption of the chromophores.[38] The orientation of SD1 will spread to adjacent LC molecules via intermolecular interactions and thus guide the LC directors. Due to the rewritability of the photoalignment agent, only the last written polarisation information will be recorded.

To perform the photopatterning, a digital micromirror device (DMD) based dynamic micro-lithography system is developed.[35] The DMD (Discovery 3000, Texas Instruments) plays the role as a dynamic mask. It consists of 1024 × 768 micro-mirrors and the size of each mirror is 13.68 μm × 13.68 μm. These mirrors can be independently tilted by an electrostatic force, thus form an 'on' or 'off' state by toggling the applied voltage. As schematically illustrated in Figure 1, a uniform and collimated beam filtered at 320–500 nm from a mercury lamp (S1000, EXFO, Canada) is reflected onto the DMD controlled by the computer. Subsequently, the bundle of light reflected by the 'on' state mirrors carries on the designed pattern. After being focused by an apo-chromatically corrected projection lens (10×, NA = 0.3, WD = 34 mm, Cinv Optics Co., China), and polarised by a motorised rotating polariser, the beam then projects onto the LC cells or glass substrates coated with SD1 placed at the image plane. A charge-coupled device (CCD) is utilised to collect the light reflected by the sample in order to monitor the focusing process. The optical path between sample and DMD is conjugated to that of sample to CCD. Owing to the excellent flexibility of image output capability of DMD, arbitrarily fine photo patterned LCs

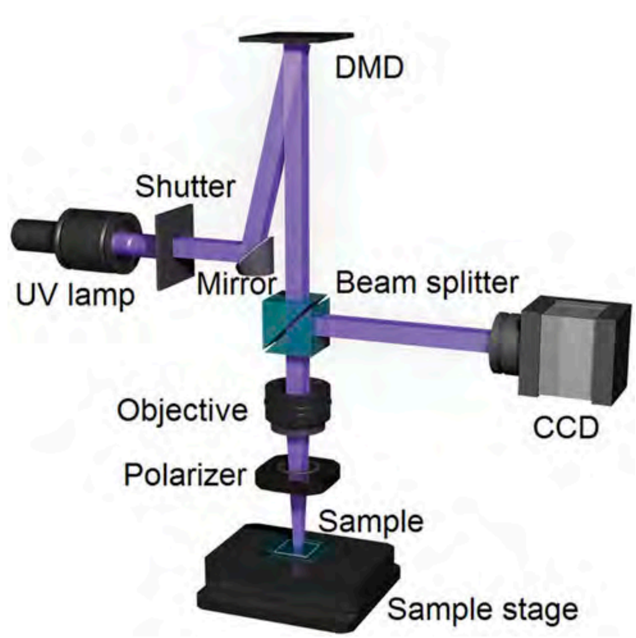

Figure 1. (colour online) Schematic illustration of the DMD-based microlithography set-up.

can be conveniently obtained, making tailoring of any structured beams possible.

3. Optical vortices generation

Optical vortices are characterised by helical phase fronts and donut-shaped intensity distributions. Their unique helical phase fronts result in an orbital angular momentum (OAM) of $m\hbar$ per photon.[5] More generally, they can be described by the so-called Laguerre–Gaussian (LG) mode with two specific indices: the topological charge m and the radial index p. The OAM of optical vortices adds a new degree of freedom to the manipulation of light, leading to applications such as optical tweezers, quantum informatics and OAM-based optical communications.

3.1. Via fork gratings

A convenient way to realise an optical vortex is via a 'fork' grating, which is a computer-generated hologram of a Gaussian beam and an optical vortex. An example with $m = 1$ is shown in Figure 2(a), it is a diffraction grating with dislocations in the centre, looking like a fork. When a Gaussian beam illuminates the fork grating, it will be diffracted into a series of optical vortices. Figure 2(b) exhibits the micrograph of a sample with $m = 1$ taken under cross-polarisers, which consists of two complementary hybrid aligned nematic (HAN) domains. One substrate of the cell is coated with SD1 and recorded orthogonally planar aligned fork grating patterns (Figure 2(a)). The pattern is realised through a two-step photo-exposure process [29] with our dynamic micro-lithography system. The other substrate is coated with a polyimide (PI-5661, Nissan, Japan) layer for vertical alignment. Comparing Figure 2(b) with Figure 2(a), the designed pattern is accurately transferred into the LC cell. The uniform colour and brightness in Figure 2(b) prove the excellent orthogonality. LC fork gratings in various alignment modes with arbitrary topological charges are fabricated.[39]

A 671 nm laser beam illuminates the sample and its diffraction patterns are captured by a CCD. Thanks to the design of orthogonal alignment, the two perpendicular components derived from all incident polarisation experience equal refractive index change, resulting in an excellent polarisation independency.[29,40] By changing the applied voltage, a maximum efficiency of 37% (74% for total ±1st orders) is obtained (ON state) as shown in Figure 2(c), when the phase retardation between the o-ray and e-ray satisfies the half-wave condition. Theoretically, the maximum diffraction efficiency for a binary phase fork grating is 40.5% for a single first order, here the obtained efficiency is close to the theoretical limitation and significantly improved compared to that generated by commercial SLMs. If proper uniform electric field is vertically applied to satisfy the full-wave condition, the ±1st orders are highly suppressed and only a none diffracted Gaussian beam can be observed (OFF state) as shown in Figure 2(d). That reveals the dynamic switching between Gaussian mode and optical vortices can be realised through electric tuning. Besides, the electrically tunable half-wave condition makes the device suitable

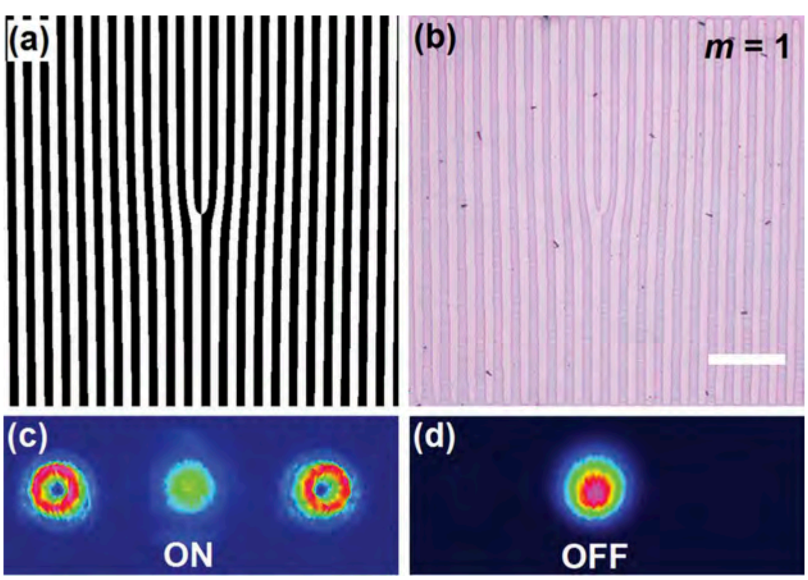

Figure 2. (colour online) (a) The computer-generated hologram of a fork grating with $m = 1$. (b) Micrograph of an orthogonal HAN LC fork grating. The cell is infiltrated with LC E7 and the scale bar is 100 μm. Corresponding diffraction patterns at (c) ON and (d) OFF state.

for a broad wavelength range. Since SD1 is optically rewritable, the pattern could be erased by a uniform linearly polarised UV light and then rewritten at optical isotropic state to obtain a new hologram. That means the mode variation is also dynamic.[39]

3.2. Via forked polarisation gratings

Though the mode conversion efficiency is improved, the diffraction efficiency for a binary phase fork grating is still quite limited. It severely restricts the applications of optical vortices. To further improve it, the Pancharatnam–Berry (PB) phase,[41] which results from the space-variant manipulation of polarisation, can be introduced. For such PB phase devices, the input energy can be totally diffracted into a single order. The LC forked polarisation grating (FPG) is proposed and demonstrated,[32,42] which can be seen as a fork grating encoded with a space-variant director distribution like a polarisation grating (PG).[43–46] The specific space-variant alignment is realised via a multi-step partly overlapping exposure.[42] The micrographs of a traditional LC PG, two FPGs with m = 2, m = 1 and p = 1, are exhibited in Figure 3(a–c), respectively. The continuous and periodic change of the brightness is caused by the spatially varying of LC directors. When rotating the samples, the dark and bright domains interconvert gradually. A disclination circle is observed in Figure 3(c) caused by the $\pi/2$ shift of the LC director astride the discontinuities.

When a Gaussian beam illuminates these samples, only three diffraction orders exist: the 0th order, a Gaussian mode with the same polarisation as the input one, and the ±1st orders, which are always circularly polarised and orthogonal to each other with OAM of opposite m. The intensity distribution between the 0th and the ±1st orders depends on the phase retardation and the incident polarisation. If the phase retardation satisfies half-wave condition, only the ±1st orders exist, and when illuminated by a left/right circularly polarised beam, only the +1st/−1st optical vortex can be obtained (theoretically, the conversion efficiency is 100%). Experimental results are shown in Figure 3(e,f), with incident polarisations labelled. Specially, for LG modes with a positive integral p, they will present $p + 1$ concentric rings as shown in Figure 3(f). A maximum efficiency of ~98.5% is achieved and the dynamic energy distribution between the ±1st optical vortices could be accomplished by changing the incident polarisation. Thanks to the excellent image-output flexibility of the dynamic photopatterning system, optical vortices carrying arbitrary azimuthal and radial indices can be generated.[42] They exhibit advantages such as extreme high conversion efficiency, polarisation controllability and electrical tunability. The polarisation controlled optical vortex could bring more possibilities to the quantum process involving both spin and orbital angular momentums.

3.3. Via meta-q-plates

The q-plate [47–50] is another attractive method for generating OAM beams. It is a PB half-wave plate

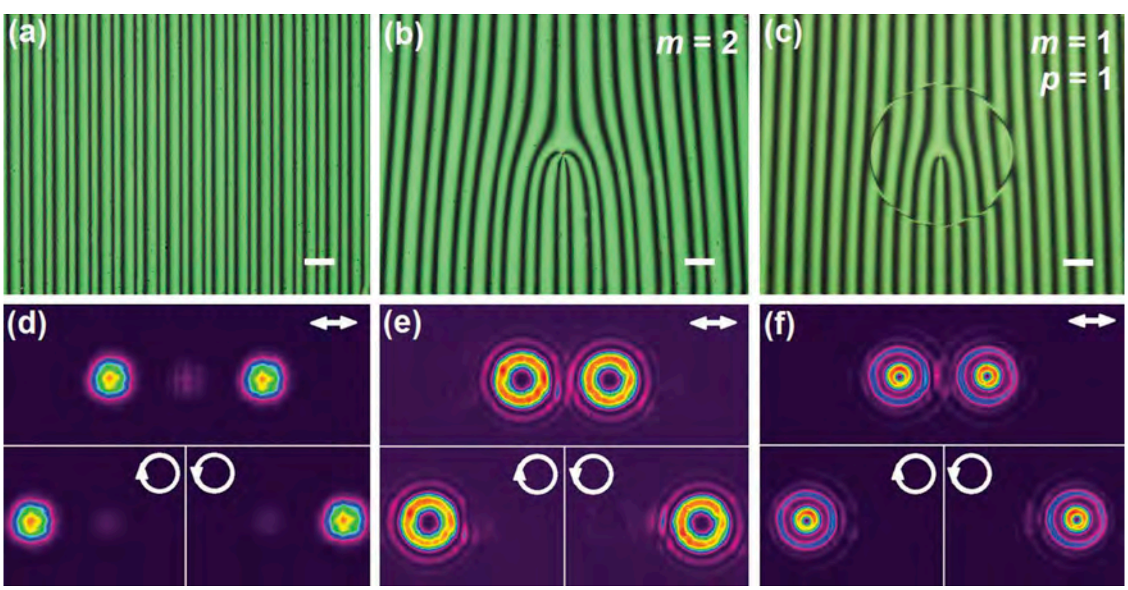

Figure 3. (colour online) Micrographs and corresponding diffraction patterns of (a), (d) an LC PG, FPGs with (b), (e) m = 2, and (c), (f) m = 1 and p = 1. All scale bars are 100 µm and incident polarisations are labelled in the images with clockwise/counter-clockwise indicating left/right circular polarisation.

with space-variant optical axis, which follows $\alpha(r, \varphi) = q\varphi+\alpha_0$, where r is the polar radius, φ is the azimuthal angle, and α_0 is the initial angle when $\varphi = 0$. The q-plates will convert circularly polarised light into an optical vortex ($m = 2q$). If q and α_0 could be arbitrarily changed along r and φ, the capability of beam shaping would be drastically enhanced and the manipulation of optical beams in a point-to-point manner is possible. We call the new concept of half-wave plate with space-variant q and α_0 as '*meta-q-plate*'.[51]

Figure 4(a,b) present the meta-q-plates with radially variant α_0 and fixed q of 1.5. Figure 4(a) is a sample with a π/2 shift of α_0 at $0.5r_0$. A circle is observed in the micrograph which is due to the disclination caused by director discontinuities. Correspondingly, a bi-ringed optical vortex with both topological charge and radial index is generated as shown in Figure 4(g). Figure 4(b) is a sample with α_0 changing from 0 to π/2 with the step of π/18 varying from the centre to the edge. The initial angle introduces an overall phase shift thus does not influence the output OAM. The final optical field pattern is still a single-ringed optical vortex in Figure 4 (h). The obtained azimuthal director distributions are examined via a two-dimensional Stokes parameters measurement and presented in Figure 4(d,e). The results indicate that the design of complex optical-axis distribution has been faithfully realised. Figure 4(c) is a sample with radially variant q and fixed $\alpha_0 = 0$. From the centre to the edge, q increases from 2 to 6.5 with an interval of 0.5. An optical field with a hurricane profile is observed. Theoretically, owing to the non-uniform intensity distribution and the rotational Poynting vector of such beam, the optical force may supply a powerful optical tweezer for complicated micromanipulations. Simulations confirm that the meta-q-plate induces a helical wavefront with spatially mixed q.[51] It might facilitate the multiplexing and demultiplexing of OAM.

3.4. Via Dammann vortex gratings

Dammann vortex grating (DVG) can provide equal-energy optical vortex beams array with specific OAMs,[11,52,53] making it possible to satisfactorily realise OAM parallel detection which is an important challenge in OAM-based optical communications. We propose a LC DVG [54] featured by alternative

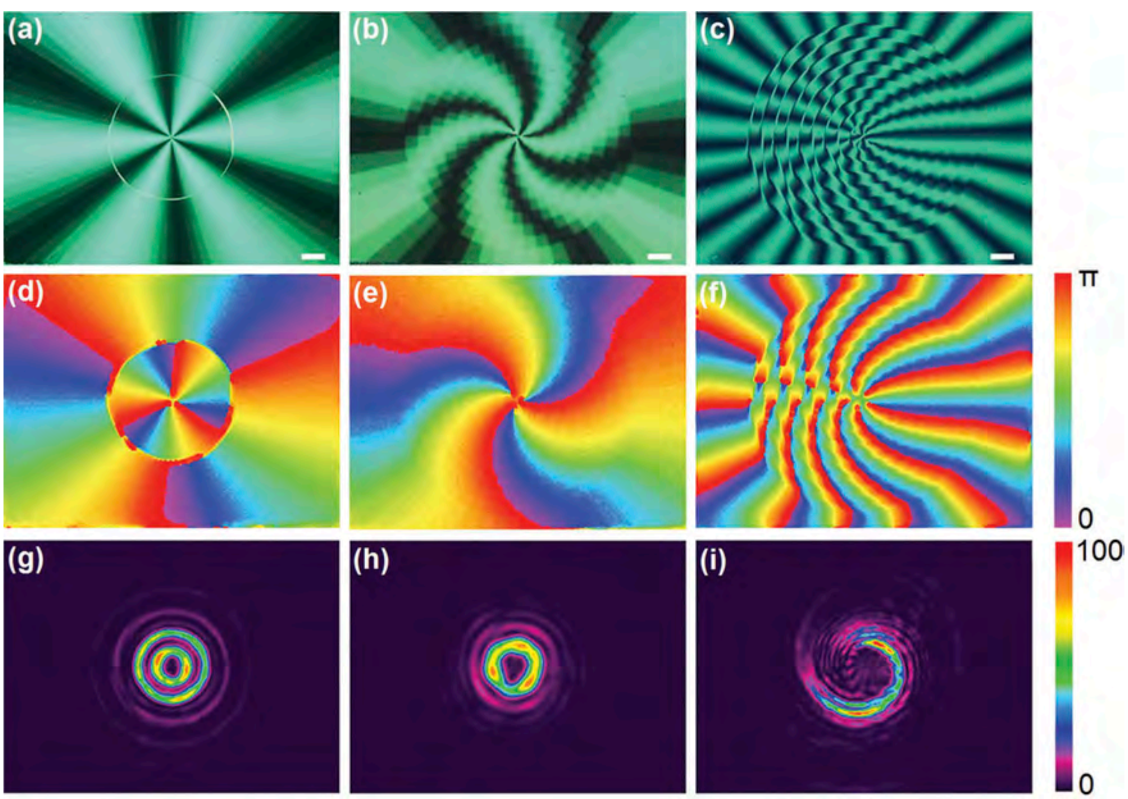

Figure 4. Micrographs, measured LC director distributions and output field patterns of meta-q-plates with (a), (d) and (g) $\alpha_0 = 0$ @ $r \leq 0.5r_0$, $\alpha_0 = \pi/2$ @ $r > 0.5r_0$, $q = 1.5$; (b), (e) and (h) $\alpha_0 = 0$ @ $r \leq 0.1r_0$, $\alpha_0 = \pi/2$ @ $r > 0.9r_0$, and from the centre to the edge, α_0 increases with an interval of π/18 every $0.1r_0$, $q = 1.5$; (c), (f) and (i) $q = 2$ @ $r \leq 0.1r_0$, $q = 6.5$ @ $r > 0.9r_0$, and from the centre to the edge, q increases with an interval of 0.5 every $0.1r_0$, $\alpha_0 = 0$. The colour bar for director distribution indicates the director varying from 0 to π, and the colour bar for output field pattern indicates the relative optical intensity.

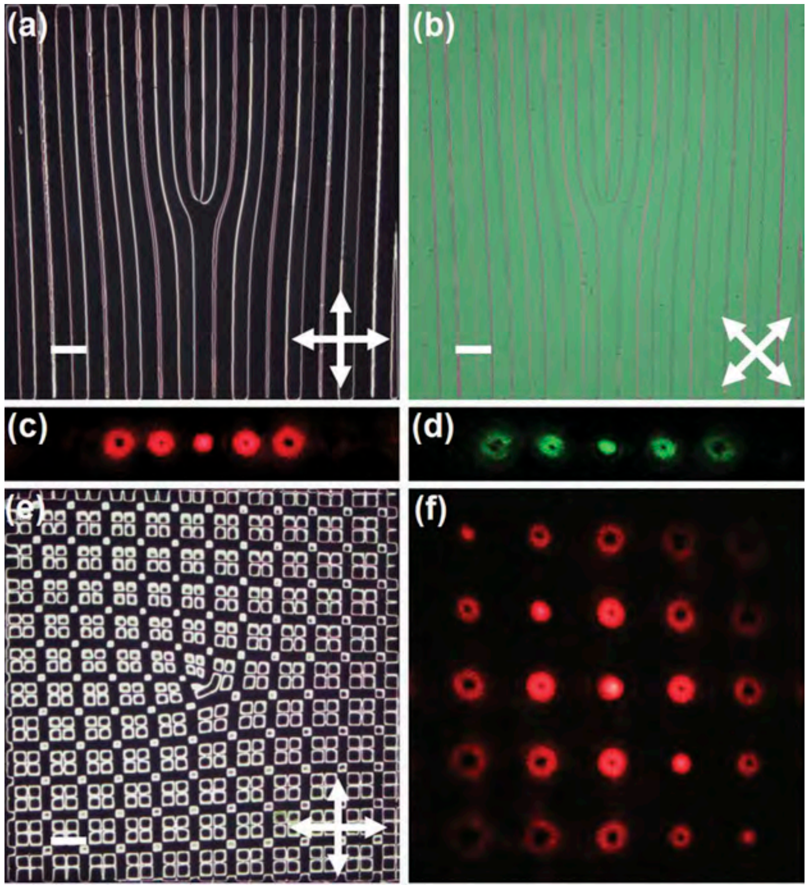

Figure 5. (colour online) Micrographs of the LC DVG with (a), (b) m = 1 and (e) m = 1 and 1. The relative directions of the polariser and analyser are labelled in white arrows. All scale bars are 100 µm. Corresponding diffraction patterns at (c), (f) 632.8 nm, and (d) 532 nm.

orthogonally planar aligned regions. Figure 5(a,b) exhibit the micrographs of a 1 × 5 LC DVG with m = 1 under different observation conditions. The diffraction patterns diffracted from a 632.8 nm laser are captured at half-wave condition and revealed in Figure 5(c). As expected, only five desired orders with similar intensities exist and the ±1st, ±2nd orders are donut-like optical vortices carrying topological charges of ±1, ±2, respectively. Thanks to the electro-optical tunability of LCs, equivalent high efficiencies could be achieved for different wavelengths by slightly tuning the applied voltages. A case for 532 nm is shown in Figure 5(d). Moreover, two-dimensional optical vortex arrays are also generated in high quality and good energy-distribution uniformity, which is verified by an example of 5 × 5 LC DVG with m = 1 and 1 as presented in Figure 5(e,f). Besides, similar to the previous orthogonal HAN fork grating, these DVGs also present excellent polarisation independence, electrical switchability and tunability. The proposed LC DVG is promising for OAM generation, manipulation and detection.

4. Vector beams generation

Optical vortex is a kind of singular beams with phase singularity, while vector beams correspond to polarisation singularity. Vector beams are featured by spatially variant polarisation states and possess a high degree of polarisation symmetry, leading to unique focusing properties thus enabling high-resolution imaging and optical manipulation.[3] We propose and demonstrate a series of LC polarisation converters suitable for arbitrary vector beam generations.[55] They are special twisted nematic (TN) cells which consist of one uniformly aligned substrate and a counter one with space-variant alignment.[26,56] Figure 6(d,e) show the polarisation converters corresponding to radially and azimuthally polarised light, with the variant polarisation distributions schematically shown in Figure 6(a,b), respectively. In our observation, the light illuminates the uniformly aligned side of the LC cell with polarisation parallel to the LC orientation. Thanks to the polarisation guiding effect, the output polarisation follows the local LC director distribution and forms the desired vector beams after going through the cell. This is verified by the intensity distributions under

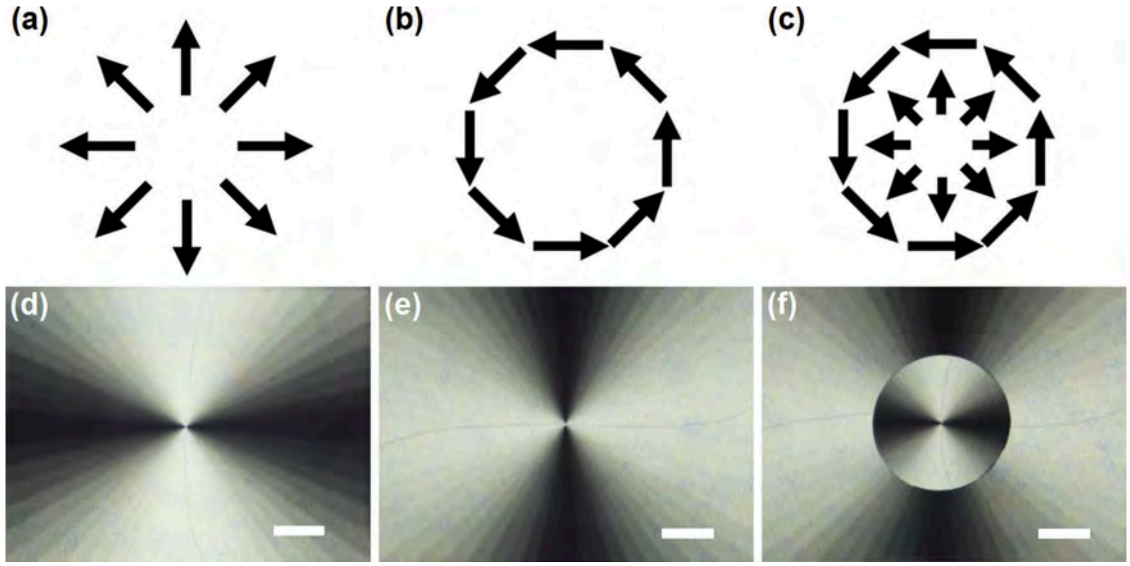

Figure 6. (colour online) The schematic polarisation and observed intensity distributions of vector beams with (a), (d) radial, (b), (e) azimuthal and (c), (f) bi-ringed polarisation. All scale bars indicate 200 μm.

the crossed-polarised microscope, where the bright and dark regions indicate the directions of local output polarisation are parallel or perpendicular to the analyser, respectively.

More complex polarisation converters can also be conveniently realised. Figure 6(f) shows an example of a bi-ringed vector beam, which possesses a bi-ringed polarisation distribution of radial and azimuthal polarisation (indicated in Figure 6(c)). The obtained converters can be further utilised as polarisation masks to implement vector-photoaligning.[55] The technique facilitates both the volume duplication of these converters and the generation of q-plates even meta-q-plates, which can convert linearly polarised laser beams into vector beams.[57] Actually, the volume duplication of any devices mentioned here can be accomplished by a one-step vector-photoaligning with specific converters.

5. Airy beams generation

Airy beam is another structured optical beam exhibiting features of non-diffraction, transverse acceleration and self-healing.[4] It has attracted considerable interest in broad fields including optical manipulation, micro-fabrication and biology science. We introduced PB phase to the design and proposed a LC polarisation Airy mask (PAM) [58] with cubically space-variant azimuthal orientations along both x- and y-axes. As shown in Figure 7(a), the brightness varies continuously. At the half-wave condition, the generated Airy beam is captured by a CCD set behind a spherical lens. For linearly polarised light, dual Airy beams appear (Figure 7(b)). For circular polarisation, only single Airy beam with orthogonal circular polarisation exists (Figure 7(d)), which matches the simulation (Figure 7(c)) perfectly. Via incident polarisation control, switch between single and dual Airy beams can be realised.

The non-diffraction and transverse acceleration features of Airy beam are well verified.[58] As the PAM here is induced by azimuthal angle control of LC, the absorptive electrodes are avoidable, therefore the optical damage threshold will be drastically increased. In our experiments, no damage was observed after 600 pulses (0.5 J/cm^2, 1064 nm, 10 ns, 1 Hz) received. Due to the limited output power of test equipment, the exact damage threshold has not been obtained yet. The value is at least one order higher than the damage threshold of commercial SLM. That means the PAM along with all above devices is promising for intense light applications such as light bullets and industrial laser processing.

6. Discussion and conclusion

Here we present a dynamic LC photopatterning technology via the combination of a polarisation-sensitive, photo-rewritable alignment agent and a dynamic micro-lithography system. This technique is suitable for implementing accurate and arbitrary azimuthal orientation control of LCs. By this means, various categories of LC devices including binary forked phase gratings, forked polarisation gratings, meta-q-plates, Dammann vortex gratings, vector beam generators and polarisation Airy masks were demonstrated. With these novel designs, vortex beams, vector beams and Airy beams were generated in high quality with unprecedented flexibility.

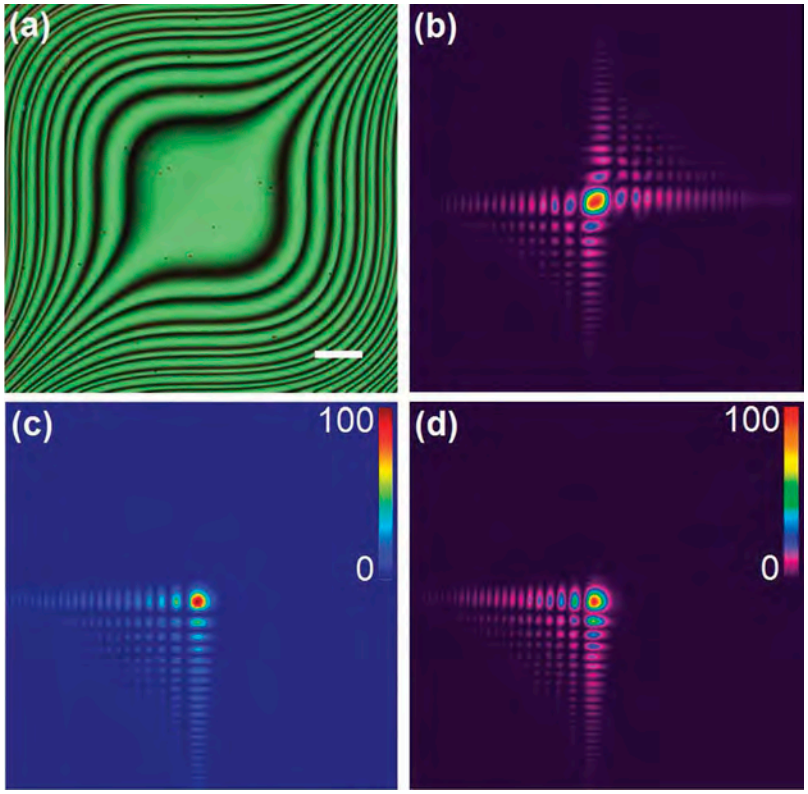

Figure 7. (a) Micrograph of an LC PAM. Intensity distributions of the generated Airy beams converted from (b) linearly and (d) circularly polarised light. The simulated result corresponding to (d) is shown in (c). The scale bar is 100 μm and the colour bar indicates the relative optical intensity.

Due to the broadband birefringence (visible, infrared to terahertz [59,60]) and electro-optical tunability of LCs, the designed microstructured LC cells can be used as versatile wavelength tunable devices, thus eliminate the cost of preparing different elements for different wavelengths. As the phase retardation can be precisely modified through adjusting the cell gap or LC birefringence, the absorptive electrodes are avoidable, making the devices applicable for short-pulse intense-light modulation. Thanks to the rewritability of SD1, the LC orientation can be reconfigured, enabling the dynamic beam shaping. Furthermore, dynamic modulation of beam profile can also be accomplished due to the electro-optical tunability of the LCs and polarisation sensitivity of certain devices. Additionally, the micro-structured LC devices exhibit merits of compact size, easy fabrication, low cost and are suitable for mass production. The technique drastically enhances the capability of optical beam shaping and steering, and settles a fundamental requirement in optics and photonics. Researches on this subject may further drive the need for optical field manipulation, and bring new opportunities in the fields of optical manipulation, high-resolution imaging, OAM-based informatics and quantum optics, and even some unchartered territories.

For most devices, the traditional nematic LC E7 is used in this work. In fact, the technique is compatible to dual-frequency [40,45] and ferroelectric LCs [61,62] as well, which can improve the switching time to sub-millisecond and even microsecond scales. Recently, with the aid of the dynamic photopatterning process, rationally designing and arbitrarily arranging the in-plane helical axes of cholesteric liquid crystals (CLCs) were realised over a scale of several centimetres.[63] The growth of some unique fingerprint textures, including spiral and wave-like continuous gratings, are demonstrated. Thanks to the intrinsic feature of CLCs, a distinctive capability of generating various featured sizes ranging from the micrometre to the submicrometre scale is provided. Besides the above cases, attempts towards new LC phases and materials is meaningful. Till now, most researches are focused on visible range, only devices with simple structures are demonstrated in telecomm band [64] and THz range.[65] Further exploiting the beam shaping extra visible range is also significant. Actually, the proposed designs could also be realised by other techniques, such as direct laser writing.[36] Meanwhile, the material for these devices is not limited to LCs, and they can also be realised in other natural or artificial birefringent materials.[66,67] Herein, only typical structured optical field of vortex beams, vector beams and Airy beams are studied. Since free control of light wavefront is possible, brand new optical fields, even holography [68] could be achievable.

Acknowledgment

The authors are indebted to Prof. V. Chigrinov for his kind support with photoalignment agent and technique.

Disclosure statement

No potential conflict of interest was reported by the authors.

Funding

This work was supported by the National Natural Science Foundation of China [grant number 11304151], [grant number 61490714], [grant number 61435008] and [grant number 61575093].

References

[1] Franke-Arnold S, Allen L, Padgett M. Advances in optical angular momentum. Laser Photonics Rev. 2008;2:299–313. doi:10.1002/lpor.200810007.

[2] Yao AM, Padgett MJ. Orbital angular momentum: origins, behavior and applications. Adv Opt Photonics. 2011;3:161–204. doi:10.1364/AOP.3.000161.

[3] Zhan Q. Cylindrical vector beams: from mathematical concepts to applications. Adv Opt Photonics. 2009;1:1–57. doi:10.1364/AOP.1.000001.

[4] Siviloglou G, Broky J, Dogariu A, et al. Observation of accelerating Airy beams. Phys Rev Lett. 2007;99:213901. doi:10.1103/PhysRevLett.99.213901.

[5] Allen L, Beijersbergen MW, Spreeuw R, et al. Orbital angular momentum of light and the transformation of Laguerre-Gaussian laser modes. Phys Rev A. 1992;45:8185–8189. doi:10.1103/PhysRevA.45.8185.

[6] Yalizay B, Soylu B, Akturk S. Optical element for generation of accelerating Airy beams. J Opt Soc Am A. 2010;27:2344–2346. doi:10.1364/JOSAA.27.002344.

[7] Beijersbergen M, Coerwinkel R, Kristensen M, et al. Helical-wavefront laser beams produced with a spiral phaseplate. Opt Commun. 1994;112:321–327. doi:10.1016/0030-4018(94)90638-6.

[8] Machavariani G, Lumer Y, Moshe I, et al. Efficient extracavity generation of radially and azimuthally polarized beams. Opt Lett. 2007;32:1468–1470. doi:10.1364/OL.32.001468.

[9] Polynkin P, Kolesik M, Moloney JV, et al. Curved plasma channel generation using ultraintense Airy beams. Science. 2009;324:229–232. doi:10.1126/science.1169544.

[10] Cao R, Yang Y, Wang J, et al. Microfabricated continuous cubic phase plate induced Airy beams for optical manipulation with high power efficiency. Appl Phys Lett. 2011;99:261106. doi:10.1063/1.3672210.

[11] Lei T, Zhang M, Li Y, et al. Massive individual orbital angular momentum channels for multiplexing enabled by Dammann gratings. Light Sci Appl. 2015;4:e257. doi:10.1038/lsa.2015.30.

[12] Yu N, Capasso F. Flat optics with designer metasurfaces. Nature Mater. 2014;13:139–150. doi:10.1038/nmat3839.

[13] Yulevich I, Maguid E, Shitrit N, et al. Optical mode control by geometric phase in quasicrystal metasurface. Phys Rev Lett. 2015;115:205501. doi:10.1103/PhysRevLett.115.205501.

[14] Zhou J, Liu Y, Ke Y, et al. Generation of Airy vortex and Airy vector beams based on the modulation of dynamic and geometric phases. Opt Lett. 2015;40:3193–3196. doi:10.1364/OL.40.003193.

[15] Yang DK, Wu ST. Fundamentals of liquid crystal devices. England: John Wiley & Sons; 2006.

[16] Schadt M. Nematic liquid crystals and twisted-nematic LCDs. Liq Cryst. 2015;42:646–652.

[17] Kitzerow H-S. Polymer-dispersed liquid crystals from the nematic curvilinear aligned phase to ferroelectric films. Liq Cryst. 1994;16:1–31. doi:10.1080/02678299408036517.

[18] Ren HW, Lin Y-H, Wu S-T. Linear to axial or radial polarization conversion using a liquid crystal gel. Appl Phys Lett. 2006;89:051114. doi:10.1063/1.2335589.

[19] Luo D, Dai H, Sun X. Polarization-independent electrically tunable/switchable Airy beam based on polymer-stabilized blue phase liquid crystal. Opt Express. 2013;21:31318–31323. doi:10.1364/OE.21.031318.

[20] Ge S-J, Ji W, Cui G-X, et al. Fast switchable optical vortex generator based on blue phase liquid crystal fork grating. Opt Mater Express. 2014;4:2535–2541. doi:10.1364/OME.4.002535.

[21] Ngcobo S, Litvin I, Burger L, et al. A digital laser for on-demand laser modes. Nature Commun. 2013;4:2289. doi:10.1038/ncomms3289.

[22] Kim J-H, Yoneya M, Yokoyama H. Tristable nematic liquid-crystal device using micropatterned surface alignment. Nature. 2002;420:159–162. doi:10.1038/nature01163.

[23] Wen B, Petschek RG, Rosenblatt C. Nematic liquid-crystal polarization gratings by modification of surface alignment. Appl Opt. 2002;41:1246–1250. doi:10.1364/AO.41.001246.

[24] Honma M, Nose T. Polarization-independent liquid crystal grating fabricated by microrubbing process. Jpn J Appl Phys. 2003;42:6992–6997. doi:10.1143/JJAP.42.6992.

[25] Chen J, Bos PJ, Vithana H, et al. An electro-optically controlled liquid crystal diffraction grating. Appl Phys Lett. 1995;67:2588–2590. doi:10.1063/1.115140.

[26] Stalder M, Schadt M. Linearly polarized light with axial symmetry generated by liquid-crystal polarization converters. Opt Lett. 1996;21:1948–1950. doi:10.1364/OL.21.001948.

[27] Schadt M, Schmitt K, Kozinkov V, et al. Surface-induced parallel alignment of liquid crystals by linearly polymerized photopolymers. Jpn J Appl Phys. 1992;31:2155–2164. doi:10.1143/JJAP.31.2155.

[28] Schadt M, Seiberle H, Schuster A. Optical patterning of multi-domain liquid-crystal displays with wide viewing angles. Nature. 1996;381:212–215. doi:10.1038/381212a0.

[29] Hu W, Srivastava AK, Lin X-W, et al. Polarization independent liquid crystal gratings based on orthogonal photoalignments. Appl Phys Lett. 2012;100:111116. doi:10.1063/1.3694921.

[30] Blinov L, Barberi R, Cipparrone G, et al. Liquid crystal orientation by holographic phase gratings recorded on photosensitive Langmuir-Blodgett films. Liq Cryst. 1999;26:427–436. doi:10.1080/026782999205209.

[31] Provenzano C, Pagliusi P, Cipparrone G. Highly efficient liquid crystal based diffraction grating induced by polarization holograms at the aligning surfaces. Appl Phys Lett. 2006;89:121105. doi:10.1063/1.2355456.

[32] Li Y, Kim J, Escuti MJ. Orbital angular momentum generation and mode transformation with high efficiency using forked polarization gratings. Appl Opt. 2012;51:8236–8245. doi:10.1364/AO.51.008236.

[33] Nersisyan SR, Tabiryan NV, Steeves DM, et al. The promise of diffractive waveplates. Opt Photonics News. 2010;21:40–45. doi:10.1364/OPN.21.3.000040.

[34] Culbreath C, Glazar N, Yokoyama H. Note: automated maskless micro-multidomain photoalignment. Rev Sci Instrum. 2011;82:126107. doi:10.1063/1.3669528.

[35] Wu H, Hu W, Hu H-C, et al. Arbitrary photo-patterning in liquid crystal alignments using DMD based lithography system. Opt Express. 2012;20:16684–16689. doi:10.1364/OE.20.016684.

[36] Miskiewicz MN, Escuti MJ. Direct-writing of complex liquid crystal patterns. Opt Express. 2014;22:12691–12706. doi:10.1364/OE.22.012691.

[37] Akiyama H, Kawara T, Takada H, et al. Synthesis and properties of azo dye aligning layers for liquid crystal cells. Liq Cryst. 2002;29:1321–1327. doi:10.1080/713935610.

[38] Chigrinov V, Pikin S, Verevochnikov A, et al. Diffusion model of photoaligning in azo-dye layers. Phys Rev E. 2004;69:061713. doi:10.1103/PhysRevE.69.061713.

[39] Wei B-Y, Hu W, Ming Y, et al. Generating switchable and reconfigurable optical vortices via photopatterning of liquid crystals. Adv Mater. 2014;26:1590–1595. doi:10.1002/adma.201305198.

[40] Lin X-W, Hu W, Hu X-K, et al. Fast response dual-frequency liquid crystal switch with photo-patterned alignments. Opt Lett. 2012;37:3627–3629. doi:10.1364/OL.37.003627.

[41] Berry MV. The adiabatic phase and Pancharatnam's phase for polarized light. J Mod Opt. 1987;34:1401–1407. doi:10.1080/09500348714551321.

[42] Chen P, Wei BY, Ji W, et al. Arbitrary and reconfigurable optical vortex generation: a high-efficiency technique using director-varying liquid crystal fork gratings. Photonics Res. 2015;3:133–139. doi:10.1364/PRJ.3.000133.

[43] Nersisyan S, Tabiryan N, Steeves D, et al. Optical axis gratings in liquid crystals and their use for polarization insensitive optical switching. J Nonlinear Opt Phys Mater. 2009;18:1–47. doi:10.1142/S0218863509004555.

[44] Du T, Fan F, Tam AMW, et al. Complex nanoscale-ordered liquid crystal polymer film for high transmittance holographic polarizer. Adv Mater. 2015;27:7191–7195. doi:10.1002/adma.201502395.

[45] Duan W, Chen P, Wei B-Y, et al. Fast-response and high-efficiency optical switch based on dual-frequency liquid crystal polarization grating. Opt Mater Express. 2016;6:597–602. doi:10.1364/OME.6.000597.

[46] Chen H, Weng Y, Xu D, et al. Beam steering for virtual/augmented reality displays with a cycloidal diffractive waveplate. Opt Express. 2016;24:7287–7298. doi:10.1364/OE.24.007287.

[47] Marrucci L, Manzo C, Paparo D. Optical spin-to-orbital angular momentum conversion in inhomogeneous anisotropic media. Phys Rev Lett. 2006;96:163905. doi:10.1103/PhysRevLett.96.163905.

[48] Slussarenko S, Murauski A, Du T, et al. Tunable liquid crystal q-plates with arbitrary topological charge. Opt Express. 2011;19:4085–4090. doi:10.1364/OE.19.004085.

[49] Nersisyan SR, Tabiryan NV, Mawet D, et al. Improving vector vortex waveplates for high-contrast coronagraphy. Opt Express. 2013;21:8205–8213. doi:10.1364/OE.21.008205.

[50] Tabirian N, Xianyu H, Serabyn E. Liquid crystal polymer vector vortex waveplates with sub-micrometer singularity. In: Proceedings of 2015 IEEE Aerospace Conference; 2015 Mar 7; Big Sky, Montana. doi:10.1109/AERO.2015.7119168.

[51] Ji W, Lee C-H, Chen P, et al. Meta-q-plate for complex beam shaping. Sci Rep. 2016;6:25528. doi:10.1038/srep25528.

[52] Liu J, Min C, Lei T, et al. Generation and detection of broadband multi-channel orbital angular momentum by micrometer-scale meta-reflectarray. Opt Express. 2016;24:212–218. doi:10.1364/OE.24.000212.

[53] Ge S-J, Chen P, Ma L-L, et al. Optical array generator based on blue phase liquid crystal Dammann grating. Opt Mater Express. 2016;6:1087–1092. doi:10.1364/OME.6.001087.

[54] Chen P, Ge S-J, Ma L-L, et al. Generation of equal-energy orbital angular momentum beams via photopatterned liquid crystals. Phys Rev Appl. 2016;5:044009. doi:10.1103/PhysRevApplied.5.044009.

[55] Chen P, Ji W, Wei B-Y, et al. Generation of arbitrary vector beams with liquid crystal polarization converters and vector-photoaligned q-plates. Appl Phys Lett. 2015;107:241102. doi:10.1063/1.4937592.

[56] Ko S-W, Ting C-L, Fuh AY-G, et al. Polarization converters based on axially symmetric twisted nematic liquid crystal. Opt Express. 2010;18:3601–3607. doi:10.1364/OE.18.003601.

[57] Naidoo D, Roux F, Dudley A, et al. Controlled generation of higher-order Poincare sphere beams from a laser. Nature Photonics. 2016;10:327–332. doi:10.1038/nphoton.2016.37.

[58] Wei B-Y, Chen P, Hu W, et al. Polarization-controllable Airy beams generated via a photoaligned director-variant liquid crystal mask. Sci Rep. 2015;5:17484. doi:10.1038/srep17484.

[59] Wu S-T. Birefringence dispersions of liquid crystals. Phys Rev A. 1986;33:1270–1274. doi:10.1103/PhysRevA.33.1270.

[60] Wang L, Lin X-W, Liang X, et al. Large birefringence liquid crystal material in terahertz range. Opt Mater Express. 2012;2:1314–1319. doi:10.1364/OME.2.001314.

[61] Srivastava A, Hu W, Chigrinov VG, et al. Fast switchable grating based on orthogonal photo alignments of ferroelectric liquid crystals. Appl Phys Lett. 2012;101:031112. doi:10.1063/1.4737642.

[62] Ma Y, Wei B, Shi L, et al. Fork gratings based on ferroelectric liquid crystals. Opt Express. 2016;24:5822–5828. doi:10.1364/OE.24.005822.
[63] Ma LL, Li SS, Li WS, et al. Rationally designed dynamic superstructures enabled by photoaligning cholesteric liquid crystals. Adv Opt Mater. 2015;3:1691–1696. doi:10.1002/adom.201500403.
[64] Wei BY, Chen P, Ge SJ, et al. Liquid crystal depolarizer based on photoalignment technology. Photonics Res. 2016;4:70–73. doi:10.1364/PRJ.4.000070.
[65] Wang L, Lin XW, Hu W, et al. Broadband tunable liquid crystal terahertz waveplates driven with porous graphene electrodes. Light Sci Appl. 2015;4:e253. doi:10.1038/lsa.2015.26.
[66] Niv A, Biener G, Kleiner V, et al. Manipulation of the Pancharatnam phase in vectorial vortices. Opt Express. 2006;14:4208–4220. doi:10.1364/OE.14.004208.
[67] Beresna M, Gecevičius M, Kazansky PG, et al. Radially polarized optical vortex converter created by femtosecond laser nanostructuring of glass. Appl Phys Lett. 2011;98:201101. doi:10.1063/1.3590716.
[68] Kim J, Li Y, Miskiewicz MN, et al. Fabrication of ideal geometric-phase holograms with arbitrary wavefronts. Optica. 2015;2:958–964. doi:10.1364/OPTICA.2.000958.